AJNR

Self-expanding nitinol stents in canine vertebral arteries: hemodynamics and tissue response.

A K Wakhloo, F O Tio, B B Lieber, F Schellhammer, M Graf and L N Hopkins

AJNR Am J Neuroradiol 1995, 16 (5) 1043-1051
http://www.ajnr.org/content/16/5/1043

Self-expanding Nitinol Stents in Canine Vertebral Arteries: Hemodynamics and Tissue Response

Ajay K. Wakhloo, Fermin O. Tio, Baruch B. Lieber, Frank Schellhammer, Michael Graf, and L. Nelson Hopkins

PURPOSE: To evaluate the hemodynamics and tissue response associated with stent placement in low-flow-velocity arteries. **METHODS:** Six self-expanding nitinol stents (5.5 mm caliber) were implanted transfemorally within the proximal segments of vertebral arteries (2.5 mm diameter) in six adult dogs during anticoagulative protection. **RESULTS:** Control angiograms demonstrated patency and 20% dilatation of all stented arteries. One artery was partially thrombosed 1 week later and subsequently showed a 50% stenosis. Throughout the observation period (4 to 9 months after stenting), the other five arteries remained patent without significant narrowing (≤15%). Small cervical muscle branches originating from the vertebral arteries within the stented segments remained patent. No major branch occlusions of the vertebrobasilar system were detected. Stent migration or kinking did not occur. MR studies of the brain 4 months after implantation revealed no infarcted areas. These findings were confirmed with brain sections. Stented artery specimens showed delayed stent dilatation. A comparison of the total mean thickness of intima covering the five 30- to 40-mm stents removed at 4, 6, and 9 months showed no significant difference (338, 332, and 389 μm, respectively). Histologic findings verified the macroscopic impression of a thicker intima at the inner curve of the stented artery segments and at the junctions of the stent filaments. The shortest (10 mm) stent had the thinnest neointimal growth (155 μm). Stented vessels showed compression of the media with atrophy, but without necrosis or perforation. Scanning electron photomicrographs revealed intact endothelial cell linings with typical elongated cells. **CONCLUSIONS:** No significant risk of thromboembolic events exists after implanting these nitinol stents in nonatherosclerotic vertebral arteries in dogs. Thicker neointimal growth after stenting may result from either low wall shear stress with possible flow separation or from changes in the shape and size of the stent, or both.

Index terms: Interventional instruments, stents; Animal studies

AJNR Am J Neuroradiol 16:1043–1051, May 1995

Vascular stents are envisioned as an alternative treatment for the occlusion of broad-based carotid artery aneurysms with preservation of the parent vessel (1, 2). In addition, these devices may be of use in the carotid or vertebral arterial system for vessel recoil or dissection after percutaneous transluminal angioplasty (3) (Mathias KD, Kempkes U, Mau A, Jäger H, "Results of Internal Carotid Artery PTA in 250 Patients," *Radiology* 1994; 190:622, abstract). Stents also may be applied to prevent the further progression of atherosclerosis by improving the hemodynamics of stenosed vessels. In principle, stents should establish a new flow conduit with stratified flow patterns, thus eliminating the regions of low and reversed local wall shear stress believed responsible for the heterogeneity of the arterial wall and progression of atherosclerotic changes (4–7).

After stent implantation, an amorphous layer of thrombus covers the stented part of the vessel (8). Gradually, this layer is progressively replaced by a smooth layer of fibromuscular

Received July 7, 1994; accepted after revision November 18.

Presented in part at the 32nd Annual Meeting of the American Society of Neuroradiology, Nashville, Tenn, May 1–7, 1994.

From the Departments of Neurosurgery (A.K.W., L.N.H.), and Mechanical and Aerospace Engineering (B.B.L.), State University of New York at Buffalo, the Department of Pathology, University of Texas Health Science Center, San Antonio (F.O.T.), and the Departments of Neuroradiology (F.S.) and Neuropathology (M.G.), University of Freiburg, Germany.

Address reprint requests to Ajay K. Wakhloo, MD, PhD, Department of Neurosurgery, State University of New York at Buffalo School of Medicine and Biomedical Sciences, 3 Gates Circle, Buffalo, NY 14209-1194.

AJNR 16:1043–1051, May 1995 0195-6108/95/1605–1043

Self-expanding nitinol stents in canine vertebral arteries: stent specifications and results

Animal	1	2	3	4	5	6
Original stent caliber, mm	5.5	5.5	5.5	5.5	5.5	5.5
Stent length, mm	30	35	40	10	30	35
Arterial diameter, mm	2.5	2.5	2.5	2.5	2.5	2.5
Maximum stenosis, %*	no stenosis	15	50	no stenosis	15	<15
Stent implanted, mo†	4	4	6	9	9	9
Final stent caliber, mm‡	5.0	4.5	4.5	4.0	3.0	4.0
Intima, μm§	180.25 ± 100.15	496.44 ± 139.75	332.79 ± 234.96	155.13 ± 76.03	531.70 ± 161.73	247.19 ± 121.00
Range, μm	16-481	163-865	16-1632	31-321	258-948	50-486
No. of measurements	89	111	115	91	64	78

* Measured on biplane digital subtracted angiograms.

† Time interval between stent implantation and removal.

‡ Measurements obtained after removal and fixation of specimens.

§ Intimal thickness (mean ± SD) of methyl methacrylate–embedded 70- to 100-μm transverse sections of stented specimens (metachromatic stain).

tissue. During the critical period of complete endothelialization, thromboembolic events may arise from the shedding of fresh thrombus. During an observation period of as long as 9 months, we evaluated the risk of thromboembolic cerebral infarction associated with self-expanding nitinol stent placement and investigated the patency of stented vessels in small canine vertebral arteries with low flow velocities. The average velocity and physiologic Reynolds number for a canine artery 3 mm in diameter are approximately 23 cm/s and 200, respectively (9), and thus comparable with values in humans. The importance of studying small-caliber stents in arteries smaller than 3 mm in diameter is the potential application of the stent device within the 2- to 3-mm arteries of the intracranial cerebrovascular system. In addition, small-caliber stents tend to undergo early thrombosis (10, 11).

Materials and Methods

Stent Implantation and Angiography

Six self-expanding nitinol (nickel titanium alloy) stents (Strecker stent, Boston Scientific, Watertown, Mass) were used in this study (Table). Five stents were 30 to 40 mm in length, and one was 10 mm in length; each had a maximum expanded caliber of 5.5 mm and 12 loops per circumference. Nitinol stents are knitted elastic, loosely connected, woven loops made of a single nitinol filament 100 μm in caliber, forming a porous tube. The nonexpanded stents were mounted on 5F angioplasty catheters using a crochet technique to provide total outer diameters of 2 mm. In this technique, a continuous thin nylon line is run along the catheter shaft from the tip of the proximal end. The nylon line affixes the stent to the balloon and is loosely attached to the catheter shaft with small polyurethane rings. After placing the stent at the target site, gradual retraction of the nylon line at the proximal end releases the stent. The stent expands from the proximal end.

Stents were implanted through a transfemoral approach within the proximal segment of one vertebral artery in six adult mongrel dogs (each weighing 15 to 20 kg). The animals received inhalation anesthetic with isoflurane during the procedure. Inner arterial diameters were calculated from biplane angiograms using the built-in software package of the digital subtraction angiography equipment (Digitron, Siemens, Erlangen, Germany). The proximal arterial segments had inner diameters of approximately 2.5 mm; therefore, a more distal positioning of the stents could not be accomplished without inducing severe intimal damage. To prevent the propagation of fresh thrombus during the procedure, intravenous heparin (100 IU/kg body weight) was administered before the device was introduced. After stenting, the animals received aspirin (80 mg per day orally) for 3 months to decrease the deposition of platelets on the stents and to prevent delayed arterial thrombosis. Angiography was performed immediately after stenting, at 1 and 3 weeks, and then at intervals of approximately 3 months.

Magnetic Resonance (MR) Imaging

To evaluate cerebral infarction from thromboembolic events, MR studies of the brain and upper cervical spinal cord were performed on a whole-body, high-field MR system using a superconductive magnet operating at 2.0 T (Bruker S 200, Karlsruhe, Germany). Semiaxial, sagittal, and coronal contiguous 3-mm T2-weighted RARE (rapid acquisition with relaxation enhancement) (12) images were obtained in all animals 4 months after stent implantation. The fast RARE spin-echo pulse sequence provides excellent T2 contrast, which makes this sequence especially sensitive for the visualization of smaller parenchymal lesions. Long repetition times of 3035 milliseconds and short echo times of 32 milliseconds were used.

Pathology

The stents were removed 4 months (n=2), 6 months (n=1), and 9 months (n=3) after implantation. To access stented vertebral arterial segments in the intervertebral foramina, the transverse processes of the lower two cervical vertebrae were removed with an oscillating saw. When the stents were removed, the vertebral and carotid arteries were flushed with saline solution through a 5F pig-tail catheter (Cook, Bloomington, Ind) positioned in the aortic arch. This procedure was carried out under barbiturate anesthesia. The animals were killed with an overdose of barbiturate and potassium chloride.

The brains were removed, perfusion-fixed, and stored in 4% formaldehyde for 10 to 20 days. Three-millimeter coronal macroscopic sections and microscopic sections were obtained to identify areas of infarction or atrophy. Sections of the brain tissue were stained with hematoxylin and eosin for light microscopy.

For the stent specimens, a longitudinal half was dehydrated and embedded in methyl methacrylate. Transverse sections of 75 to 100 μm were obtained with an isomet low-speed rotary diamond saw (Bühler, Lake Bluff, Ill) and stained with metachromatic stain. For scanning electron microscopy, the stented vessel segments were flushed with 5% dextrose in water, treated with 0.25% silver nitrate in 5% dextrose in water for 10 seconds, rinsed in 5% dextrose in water, and then exposed to sunlight (10). After silver staining, the stented segments were fixed in 2% glutaral, dehydrated with alcohol, sublimated with Pel-Dri II (Ted Pella, Redding, Calif), and coated with gold-palladium for study under the scanning electron microscope (JSM 840A; Jeol USA, Peabody, Miss).

Multiple measurements of the intimal thickness of the stained transverse sections (Table) were obtained using a digitizing board (Hewlett-Packard, San Diego, Calif) and morphometric software (Sigma Scan, Jandel Scientific, San Rafael, Calif).

Results

Angiography

Postprocedural angiograms showed patency and an approximately 20% dilatation of all stented canine vertebral arteries. No dissection, early thrombus formation, or significant vasospasm was noted. One artery was partially thrombosed 1 week after implantation and subsequently showed a 50% stenosis (animal 3). Angiograms performed in the other animals at 4 and 9 months showed patent vessels without significant stenosis. Although blood flow was reduced in the major smaller cervical branches originating from the vertebral arteries within the stented segments, these branches remained patent during the observation period (Fig 1). No major branch occlusions of the intracranial or extracranial vertebrobasilar arterial system were detected. No migration, kinking, or material fractures of the stents were seen on nonsubtracted x-ray images.

MR Imaging

The MR images, including images from animal 3, were not suggestive of brain infarction or injury of the upper cervical spinal cord. No focal or generalized atrophy of brain or spinal cord tissue was observed.

Pathology

The MR findings were substantiated by macroscopic and light microscopic investigations. Neither atrophy nor infarction of cortical, deep white, or gray matter was detected in any brain specimens, including specimens from animal 3. No organized thrombus was found in the larger vessel of the circle of Willis or intracranial segment of the vertebrobasilar system.

Macroscopic investigation of the vascular tissue surrounding the stented segments did not reveal inflammatory reaction or substantial fibrotic tissue reaction. Nitinol filaments were visible through the almost translucent vessel walls, which appeared stretched and thin. The fixed vessels showed delayed expansion of the stent, measuring 3.0 to 5.0 mm. Specimens removed at 4 months were completely covered with a smooth, 338-μm intimal layer (mean value), whereas those removed at 9 months (Fig 2) had a 389-μm intimal layer (data from animal 4, 10-mm stent, excluded). In the single partially thrombosed and stenosed stent removed from animal 3, webs of fibromuscular neointima traversed the lumen. The average intimal thickness of that sample was 332 μm, which was less than the mean intimal thickness found in one of the 4-month specimens (animal 2). A comparison of the total mean thickness of intima covering the five 30- to 40-mm stents removed at 4, 6, and 9 months showed no significant difference (338, 332, and 389 μm, respectively).

Microscopic findings verified the macroscopic impression of a thicker intimal proliferation at the inner bend of the curved stented vessel segments (Fig 3). Neointimal growth was more expressed at the junction of filaments, even if the struts were completely interlocked, (ie, no openings existed between filaments). Stented vessels showed compression and atro-

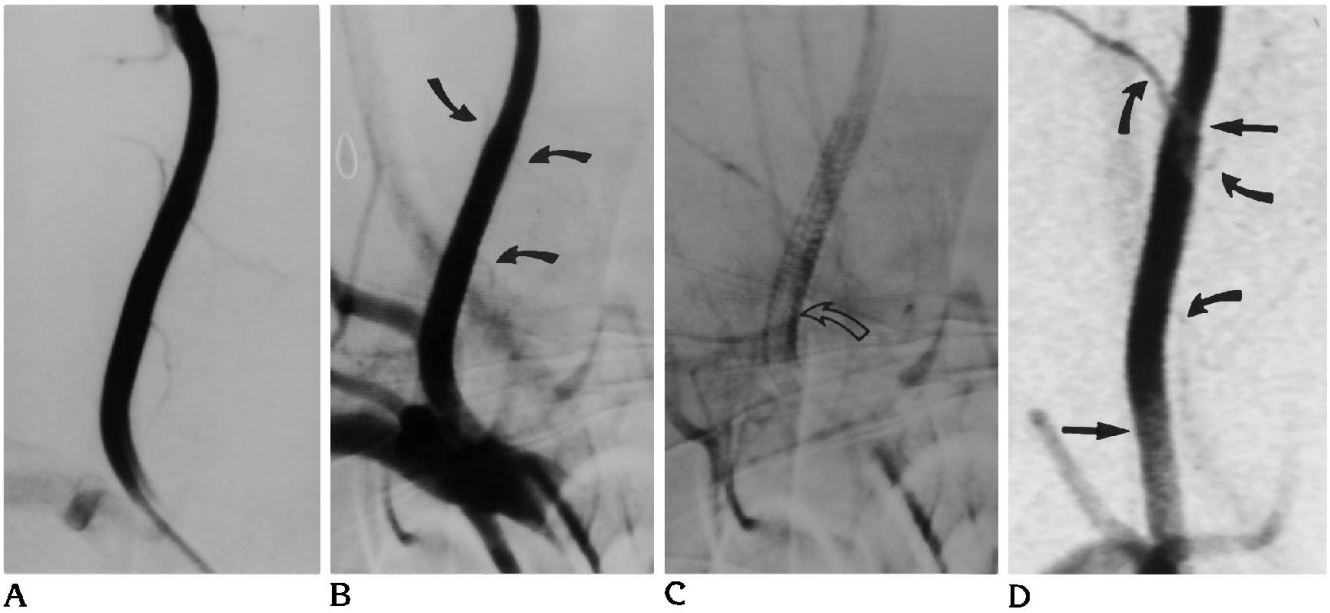

Fig 1. Animal 6 (Table). *A*, Anteroposterior angiogram of the right vertebral artery before stent placement. The proximal diameter of the vessel is approximately 2.5 mm. Major smaller cervical muscle branches are well delineated.

B, Angiogram (same projection) obtained immediately after transfemoral implantation of a nitinol type I stent 35 mm in length with a 5.5-mm caliber shows the stent molded against the vessel wall with approximately 20% overdilatation of the artery to a diameter of 3.0 mm. The cervical muscle branches traversed by the stent demonstrate angiographic patency (*curved arrows*).

C, Late arterial phase (same projection) shows that part of the contrast material is trapped between the stent filaments with delayed washout, more so at the inner curve of the stented segment (*open arrow*).

D, Follow-up angiogram (oblique projection) obtained 9 months after stent placement demonstrates no significant narrowing of the stented segment (*arrows*). Major smaller cervical muscle branches covered by the stent are still visible (*curved arrow*), and delayed flow was observed (not shown).

phy of the media and increased intimal thickening in the central portions of stented vessel segments, resulting from areas of maximal radial force. Decreased radial force at the proximal and distal site of the stent resulted in less intimal thickening. However, neither necrosis nor perforation of the medial layer was detected (Figs 2 and 3). No inflammatory or foreign-body reaction was noticed in either layer of the vessel wall. Scanning electron micrographs showed endothelial cell linings with typical elongated cells and their protruding nuclei (Fig 2).

Discussion

Stent Material Properties

Preliminary successful results with the self-expanding nitinol Strecker stents to treat side wall aneurysms in canine carotid arteries (2) motivated continued experimentation using these devices. Nitinol stents possess excellent flexibility and adapt easier to the vessel course than tantalum stents (11).

Nitinol is an equiatomic alloy composed of nickel and titanium. The molecular properties of nitinol allow it to exist in two different states, depending on its temperature. At a lower temperature, the alloy assumes a state, known as the *martensite phase*, in which it is more flexible and malleable. When heated above a certain transformation temperature, it reforms into a predetermined annealed, or austentite, shape. By slightly altering the composition of the alloy, the transformation temperature can be altered. During the martensite phase, a nitinol stent can be compressed and delivered through a small vascular sheath. On reaching its target site, the stent is extruded into the blood stream where, at body temperature, the filament resumes its predetermined annealed shape. However, this material property was not used in the current study.

Fig 2. Animal 6 (Table). *A*, Longitudinal section of a stented vertebral artery removed 9 months after stenting (approximate diameter of fixed stent segment is 4.0 mm). Note the increased intimal thickening at the junction of stent filaments, regardless of existing interfilament gaps (*arrows*). *White arrows* indicate blood flow direction.

B, Photomicrograph of the methyl methacrylate–embedded transverse section of nitinol stent (original magnification × 10, metachromatic stain) shows thin intima. Note distinct stretching, compression, and atrophy of medial layer (*curved arrows*).

C, Scanning electron photomicrograph shows a uniform intimal layer covering the nitinol filaments (SEM, original magnification × 20). Artificial cracks are seen in the intima.

D, Scanning electron photomicrograph displays complete endothelial cell lining with typical elongated cells and their protruding nuclei but no desquamation (SEM, original magnification × 500).

The tantalum Strecker stent (Boston Scientific, Jyllingen, Denmark) is made of 99% tantalum. Tantalum is a highly radiopaque material. Tantalum and nitinol stents are biocompatible, nonferromagnetic, and resistant to corrosion, abrasion, and oxidation (13, 14).

The advantages of the nitinol stent for intravascular application are ease of delivery, high expansion ratio (ie, expanded diameter-to-constrained diameter), and reliable expansion. Unlike the tantalum and stainless steel Palmaz stents (Johnson & Johnson Interventional Systems, Warren, NJ), nitinol stents do not require a balloon angioplasty catheter for implantation, which reduces the risk of intimal injury leading to increased platelet aggregation and intimal hyperplasia. The self-expanding nitinol stent possesses high elasticity compared with the balloon-expandable tantalum stent, which shows plastic deformation and may recoil. Recoiling increases the amount of thrombus formation and subsequent arterial narrowing of stented vessel segments because of neointimal growth (2). When stainless steel stents were placed in swine iliac arteries, proliferative reactions were more remarkable in vessels containing balloon-expandable stents than in vessels containing self-expanding stents (15). Stent porosity (ratio of metal to tissue) is another factor associated with neointimal growth. In rabbit arteries, spiral-shaped nitinol stents without gaps induced a pronounced neointimal growth compared with stents with gaps (16). Thus, a small metal-to-tissue ratio appears to play an important role in preventing excessive neointimal growth.

Hemodynamics

We were able to insert safely Strecker nitinol stents in canine vertebral arteries smaller than 3 mm in diameter. Other investigators (17, 18) have reported that stent implantation within small (3 mm) arteries of low blood-flow velocity is associated with a higher rate of early thrombosis. We found no significant risk of microembolization or cerebral infarction after stenting proximal vertebral arteries in dogs. Although early thrombosis of the stent occurred, rapid endothelialization of the thrombus minimized microembolization. Any early microemboli were apparently lysed by the active fibrinolytic system in dogs (19, 20). No occlusion of the proximal vertebral arteries occurred, and no regional collateral circulation was seen on the digitally subtracted angiograms. However, smaller branches are difficult to evaluate because of the complexity of the canine cervical vasculature.

In recent reports of patients treated with tantalum stents and stainless steel balloon-expandable stents (Palmaz stents) for atherosclerotic disease and aneurysms of the internal

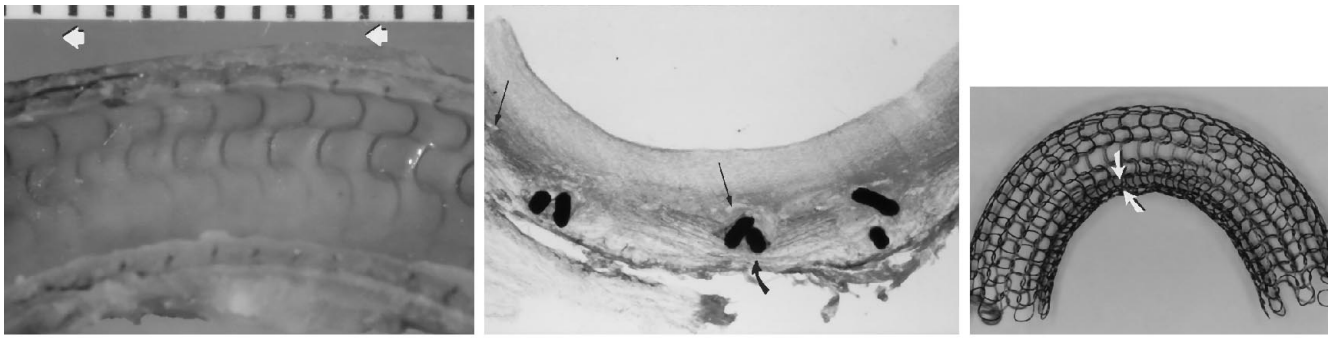

Fig 3. Animal 2 (Table). *A*, Longitudinal macroscopic view of a more curved portion of vertebral artery segment removed 4 months after stent placement shows a smooth but much thicker layer of intima than in Figure 2, especially at the inner curve of the vessel (caliber of stent in fixed vessel segment, approximately 4.5 mm). *Arrows* indicate blood flow direction.

B, Methyl methacrylate–embedded transverse section (original magnification × 10; metachromatic stain) shows compression of the subjacent tunica media and disruption of the elastic membrane but no compression necrosis or perforation of the arterial wall (*curved arrow*). The histology of stent-intima interface is fairly bland with residual hemosiderin pigments and few capillaries around the stent (*arrows*), but no significant inflammatory cell reaction is present and no multinucleated giant cells are identified.

C, Close-up photograph of a fully expanded stent, maintained in a flexed position through external force. The filaments at the inner bend of the stent tend to project into the lumen because of longitudinal shortening and intrinsic rigidity of the woven structure (*arrows*).

carotid artery, no clinical signs of cerebral infarction were associated with cervical stent implantation during an observation period of more than 6 months (1) (Mathias et al, "Results").

The principal advantage of the nitinol stent lies in its flexibility, which allows it to conform to the tortuousity of blood vessels. Stent flexibility also avoids the enhanced intimal thickness and early occlusion associated with kinking at transitional zones of the stent. Compared with the Palmaz stent, however, the nitinol stent has been shown to have less resistance to elastic deformation (ie, a smaller elasticity modulus) (21) and may be more apt to recoil in degenerative arteries with extensive calcified plaques.

The Palmaz stent is less flexible than the nitinol stent. This disadvantage was overcome by the development of the Palmaz-Schatz stent, which has a small and flat stainless steel bridge between its two segments. However, because the bridge is rigid, the stent may not be capable of alignment to more curved arterial segments. Therefore, the Palmaz-Schatz stent may be subject to restenosis through intimal growth over the underlying atherosclerotic vessel at the junction of the two segments.

The mean neointimal proliferation in small vertebral arteries was significantly thicker than that observed in the larger canine carotid arteries (2), and angiograms showed insignificant (≤15%) stenosis, except in animal 3 (50% stenosis). The inner bends of curved stented segments have thicker neointimal layers. Low or reversed wall shear stress may have promoted this tissue response (5–7). A recent study using computational methods for simulating steady flow in end-to-side straight vessel anastomoses has suggested that regions of low wall shear stress with a possible flow separation may promote the intimal hyperplasia (22). An additional explanation for the thicker neointima at the inner bend of the curved vessel segments is the compression of individual loops, which is clearly apparent when the stent is flexed. The longitudinal (axial) compression of the stent at the inner bend also forced the woven loops between junctions to project into the vessel lumen (Fig 3C), causing enhanced thrombus formation. This may be prevented by the design of a porous unibody nonwoven stent that possesses high flexibility and resists elastic deformation.

Low-flow velocity profile also is an important hemodynamic parameter. Low-flow velocity augments neointimal growth in smaller vessels (23, 24). Although only one short (10 mm) nitinol stent was implanted (Table, animal 4), our data revealed a beneficial effect of the straight shorter stent on the amount of intimal growth. This stented segment had a uniform and the thinnest intimal cover (average thickness, 155 μm). These observations emphasize the importance of stent design and local hemodynamics in determining eventual neointimal thickness. At this point, we can only speculate that an increased intimal thickness was found at the junction of stent filaments because of stag-

nant flow, which induces a larger amount of thrombus deposition.

Transverse histopathologic sections of the stented vessels revealed markedly stretched media with disrupted internal elastic membranes. This resulted from overdilating the arteries to more than twice their original diameters (stent-to-artery ratio was 2.2:1) and from delayed expansion caused by the persistent radial force of the self-expanding stents. Stretching of the media also may cause proliferation of myofibroblasts, which further contributes to the stenosis (25, 26). We observed that the neointimal tissue covering the central stented portion of the artery, associated with higher radial force exerted by the stent, was thicker in animal 4. There was compression atrophy of the media, but no perforation was detected. The early closure of one stented vertebral artery (animal 3) may have been caused by oversizing the stent. Oversized stents resulting in abrupt changes in luminal diameter also have been reported to promote early occlusion (Puel J, Sigwart U, Joffre F, et al, "Percutaneously Implantable Endocoronary Prosthesis: Preliminary Results in the Treatment of Post-dilatation Re-stenosis," *J Am Coll Cardiol* 1987; 9 [suppl]: 106A, abstract) (Sigwart U, Grbic M, Essinger A, Kappenberger L, "First Follow-up Data on the Transluminally Implanted Coronary Endoprosthesis," *J Am Coll Cardiol* 1987; 9 [suppl]: 106A, abstract), yet Roubin et al (27) encountered none of these problems in their more current studies. Disturbance of the axial laminar flow caused by the altered hemodynamics with relative stasis and eddy formation in the dilated stent most likely had a role in the initiation of the occlusion. Why some stents progress to significant occlusion, whereas others appear to endothelialize thrombus and remain patent, is unclear. The proper titration of anticoagulants could be an important factor. Numerous studies have previously emphasized the importance of anticoagulation to prevent early stent occlusion (18, 28) (Palmaz JC, Garcia O, Kopp DT, et al, "Balloon-Expandable Intraarterial Stents: Effect of Anticoagulation on Thrombus Formation," *Circulation* 1987; 76[suppl 4]:45, abstract).

Our study is comparable to studies of stent devices in coronary arteries, which have generally been favorable. A low complication rate was reported by Levine et al (28) with balloon-expandable Palmaz-Schatz stents in coronary artery stenosis. Of 37 treated cases, 1 case of early thrombosis was encountered, and no immediate stent occlusion was observed. High rates of restenosis were found in 57% of patients with multiple stents implanted in tandem, compared with a 17% rate of restenosis in patients treated with a single stent. Although a high success rate of stent placement (95%) was reported, some stents had neointimal layers up to 680 ± 260 μm, which corresponded to stenoses of $29\% \pm 15\%$. Experiments with the recently developed balloon-expandable Gianturco-Roubin (book binder–shaped) stents have shown loss of endothelial cells and fragmentation of the internal elastic lamina with stretching of the media in the coronary arteries of dogs (27). Dogs are frequently used because of the close similarity of the coronary vasculature and hemostatic parameters to those of humans (20, 29). In those experiments (27), only $10\% \pm 6\%$ stenosis was observed 12 months after stenting the canine coronary artery (3 mm), and the side branches remained patent. Endothelialization occurred at 2 weeks, and no difference was observed between the tissue of the stented arteries examined at 2, 6, and 12 months. The histologic changes in dogs treated with warfarin compared with those treated with aspirin and dipyridamole were similar.

Limitations

The present nitinol stent has technical and design limitations. Under fluoroscopy, the poor visualization of nitinol, compared with tantalum or platinum, may contribute to imprecise positioning and also may cause the operator to select an unnecessarily longer stent. The lack of a protective sheath between the stent, delivery catheter, and the vessel wall poses a risk of intimal damage and dislodging of mural thrombi and atherosclerotic plaque. For extremely tortuous vessels, the caliber of the current stent delivery system may be a limiting factor. Further developments should aim to increase radiopacity, reduce the size of the device (including the caliber of the filaments), and improve the delivery technique.

Future testing should investigate the use of stents in atherosclerotic cerebral arteries after percutaneous transluminal angioplasty. Currently, a minimum diameter of approximately 2 mm is necessary to traverse high-grade stenotic atherosclerotic lesions with the Palmaz-Schatz or the nitinol stent. Thus, angioplasty would be

required before these stents are implanted in high-grade stenosed vessels. Both the risk from the shedding of plaques during the stenting of extensive calcified atherosclerotic arteries and the increased risk of acute thrombosis after stenting must be evaluated in a large population. In addition, residual stenosis after stent placement may promote the occurrence of restenosis caused by insufficient flow in smaller atherosclerotic arteries as compared with stenting of healthy arteries. Preliminary studies in patients with flexible stents suggest that long-term patency can be achieved in atherosclerotic coronary, peripheral, and internal carotid arteries that have previously restenosed or dissected after balloon dilatation if high flow velocity is maintained in the vessel (3, 30) (Mathias et al, "Results").

Stents cannot be used at present to treat cranial aneurysms with acute subarachnoid hemorrhage because of the need for anticoagulation. However, modification of the thrombogenic property of the stents (eg, heparin coating) may obviate anticoagulation and allow the use of stents to manage this condition (Sutton CS, Consigny PM, Thakur M, "Thrombogenicity of Intravascular Stent Wires," *Circulation* 1994; 90:1–9, abstract).

Conclusions

Our experimental results demonstrate that self-expanding nitinol stents can be placed safely into the canine vertebral artery using the transfemoral approach. The technical problems of balloon-expandable stents, such as recoil and insufficient dilatation with an undersized stent that are associated with early thrombosis and thicker neointima, can be overcome by using an oversized, self-expandable stent. With the oversized stent used in the present study, patency was maintained for 4 to 9 months. Reduced flow to the major smaller cervical branches was angiographically observed, but no occlusion of those branches occurred in the 9-month follow-up period. None of the presently available stents meet all requirements for the treatment of different arterial diseases, that is, flexibility for more tortuous vessel segments, or stiffness for heavily calcified atherosclerotic plaque. Thus, stents should be selected on an individual basis.

Acknowledgment

We thank E. P. Strecker, MD, and B. Schneider, MD, for introducing us to the crochet technique.

References

1. Marks MP, Dake MD, Steinberg GK, Norbash AM, Lane B. Stent placement for arterial and venous cerebrovascular disease: preliminary experience. *Radiology* 1994;191:441–446
2. Wakhloo AK, Schellhammer F, de Vries J, Haberstroh J, Schumacher M. Self-expanding and balloon-expandable stents in the treatment of carotid aneurysms: an experimental study in a canine model. *AJNR Am J Neuroradiol* 1994;15:493–502
3. Théron J. Angioplasty of brachiocephalic vessels. In: Viñuela F, Halbach VV, Dion JE, eds. *Interventional Neuroradiology: Endovascular Therapy of the Central Nervous System*. New York: Raven Press, 1992:167–180
4. Boussiouny HS, Lieber BB, Giddens DP, et al. Differential effect of wall shear stress on intimal thickness in critical and subcritical stenosis. *Arteriosclerosis* 1988;8:A617–A618
5. Lieber BB, Giddens DP, Zarins CK, Glagov SG. Pulsatile near wall studies distal to coarctations. In: Lantz SA, King AI, eds. *Advances in Bioengineering. The Bioengineering Division*, Vol 2. New York: ASME Publication, 1986:152–153
6. Lieber BB, Giddens DP. Post-stenotic core flow behaviour in pulsatile flow and its effects on wall shear stress. *J Biomech* 1990; 23:597–605
7. Rittgers SE, Karayannacos PE, Guy JF, et al. Velocity distribution and intimal proliferation in autologous vein grafts in dogs. *Circ Res* 1978;42:792–801
8. Palmaz JC. Intravascular stents: tissue-stent interactions and design considerations. *AJR Am J Roentgenol* 1993;160:613–618
9. Whitmore RL. *Rheology of the Circulation*. Oxford: Pergamon, 1968:92
10. Palmaz JC, Windeler SA, Garcia F, et al. Balloon expandable intraluminal grafting of atherosclerotic rabbit aortas. *Radiology* 1986;160:723–726
11. Strecker EP, Liermann D, Barth KH, et al. Expandable tubular stents for treatment of arterial occlusive diseases: experimental and clinical results. *Radiology* 1990;175:97–102
12. Hennig J, Friedburg H. Clinical applications and methodological developments of the RARE technique. *Magn Res Med* 1988;6: 391–395
13. Putters JL, Kaulesar Sukul DM, de Zeeuw GR, Bijma A, Besselink PA. Comparative cell culture effects of shape memory metal (nitinol), nickel and titanium: a biocompatibility estimation. *Eur Surg Res* 1992;24:378–382
14. Simon M, Kaplow R, Salzman E, Freiman D. A vena cava filter using thermal shape memory alloy: experimental aspects. *Radiology* 1977;125:89–94
15. Chuapetcharasopon C, Wright KC, Wallace S, Dobben RL, Giantturco C. Treatment of experimentally induced atherosclerosis in swine iliac arteries: a comparison of self-expanding and balloon-expanded stents. *Cardiovasc Intervent Radiol* 1992;15:143–150
16. Tominaga R, Harasaki H, Sutton C, Emoto H, Kambic H, Hollman J. Effects of stent design and serum cholesterol level on the restenosis rate in atherosclerotic rabbits. *Am Heart J* 1993;126: 1049–1058
17. Schatz RA, Baim DS, Leon M, et al. Clinical experience with the Palmaz-Schatz coronary stent: initial results of a multicenter study. *Circulation* 1991;83:48–161

18. Serruys PW, Strauss BH, Beatt KJ, et al. Angiographic follow-up after placement of a self-expanding coronary artery stent. *N Engl J Med* 1991;324:13–17
19. Sauvage LR, Berger KE, Wood SJ, et al. Interspecies healing of porous arterial prostheses. *Arch Surg* 1974;109:698–705
20. Bentinck-Smith J. A roster of normal values. In: Kirk RW, ed. *Current Veterinary Therapy: Small Animal Practice*. Philadelphia: Saunders, 1977; VI:1355–1359
21. Lossef SV, Lutz RJ, Mundort J, Barth KH. Comparison of mechanical deformation properties of metallic stents with use of stress-strain analysis. *J Vasc Interv Radiol* 1994;5:341–34
22. Kim YH, Chandran KB. A numerical study of steady flow across end-to-side vascular bypass graft anastomoses. *Adv Bioengineer, ASME* 1992;22:233–236
23. Palmaz JC, Garcia OJ, Schatz RA, et al. Placement of balloon-expandable intraluminal stents in iliac arteries: first 171 procedures. *Radiology* 1990;174:969–975
24. Nödge G, Richter GM, Siegerstetter V, Garcia O, Palmaz JC. Tierexperimentelle Untersuchungen über den Einfluß der Flußrestriktion auf die Thrombogenität des Palmaz-Stentes mittels ^{111}Indium-markierter Thrombozyten. *RÖFÖ Fortschr Röntgenstr* 1990; 152:264–270
25. Duprat G, Wright KC, Charnsangavej C, Wallace S, Gianturco C. Flexible balloon-expanded stent for small vessels. *Radiology* 1987;162:276–278
26. Duprat G, Wright KC, Charnsangavej C, Wallace S, Gianturco C. Self-expanding metallic stents for small vessels: an experimental evaluation. *Radiology* 1987;162:469–472
27. Roubin GS, Cannon AD, Agrawal SK, et al. Intracoronary stenting for acute and threatened closure complicating percutaneous transluminal coronary angioplasty. *Circulation* 1992;85:916–927
28. Levine MJ, Leonard BM, Burke JA, et al. Clinical and angiographic results of balloon-expandable intracoronary stents in right coronary artery stenoses. *J Am Coll Cardiol* 1990;16:332–339
29. Wintrobe MM. *Hemostasis and Blood Coagulation in Man*. 8th ed. Philadelphia: Lea & Febiger, 1981:1889
30. Palmaz JC, Laborde JC, Rivera FJ, Encarnacion CE, Lutz JD, Moss JG. Stenting of the iliac arteries with the Palmaz stent: experience from a multicenter trial. *Cardiovasc Intervent Radiol* 1992;15:291–297